

Electronic Supplementary Information for

## Spontaneously assembly of strong and conductive graphene-polypyrrole aerogel for energy storage

Rui Sun,<sup>a,b</sup> Hongyuan Chen,<sup>b</sup> Qingwen Li,<sup>b</sup> Qijun Song<sup>\*,a</sup> and Xuetong Zhang<sup>\*,b,c</sup>

\*Corresponding Author: qsong@jiangnan.edu.cn; zhangxtchina@yahoo.com

### Figures

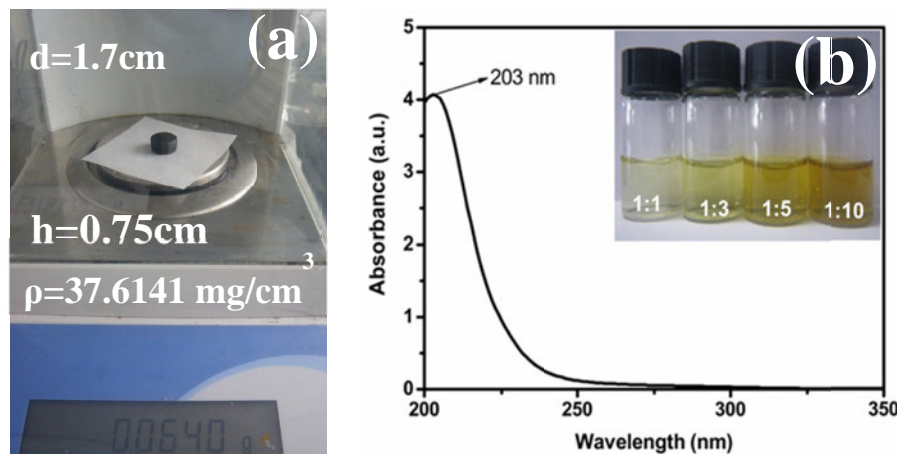


Fig. S1 (a) Photograph of rGO-PPy aerogel (PG5); (b) UV-Vis absorption spectra of the yellow solution gathered from reaction system.

The peak at 203 nm in the the UV-Vis absorption spectrum is corresponding to the character absorbance of pyrrole oligomers reported before,<sup>1, 2</sup> which demonstrates limited pyrrole is polymerized by graphene oxide. Pyrrole would be completely polymerized and newly generated PPy anchored on rGO nanosheets in the reaction system where the mass ratio of GO to Py is above 1:1.

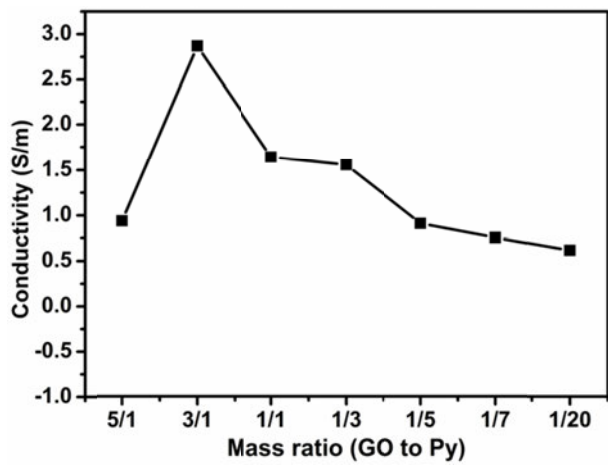


Fig. SI2 Conductivity of rGO-PPy aerogels.

The conductivity of rGO-PPy aerogels was evaluated by four point probe tester. GP5 aerogel exhibits the conductivity of 0.97 S/m due to uncompletely reduction of GO. With the increasing of Py, GO is further reduced by more Py monomers, which results higher conductivity of GP3 (2.87 S/m). However, PPy would not be doped by proton dissociation from GO if more Py added in to reaction mixture. Thus, GP1, GP3, GP5, GP7 and GP20 shows conductivity with the value of 1.65, 1.56, 0.91, 0.75, 0.61 S/m respectively.

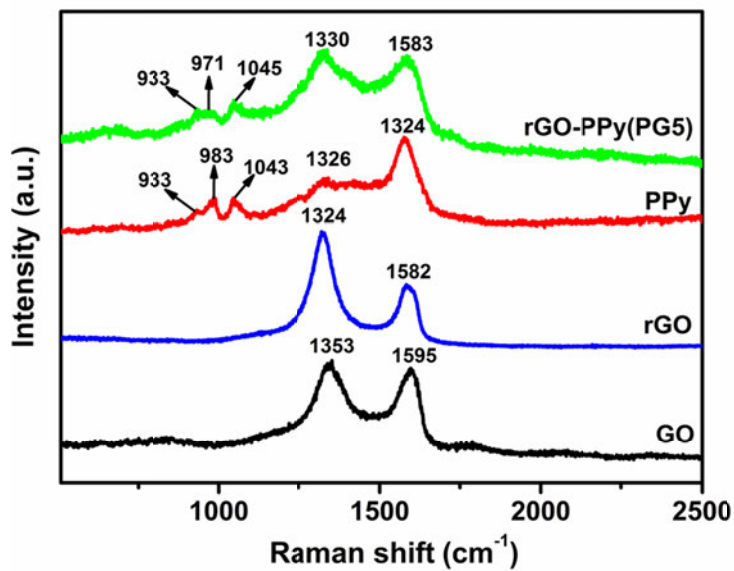


Fig. SI3 Raman spectra of GO, rGO, pure PPy and rGO-PPy aerogels.

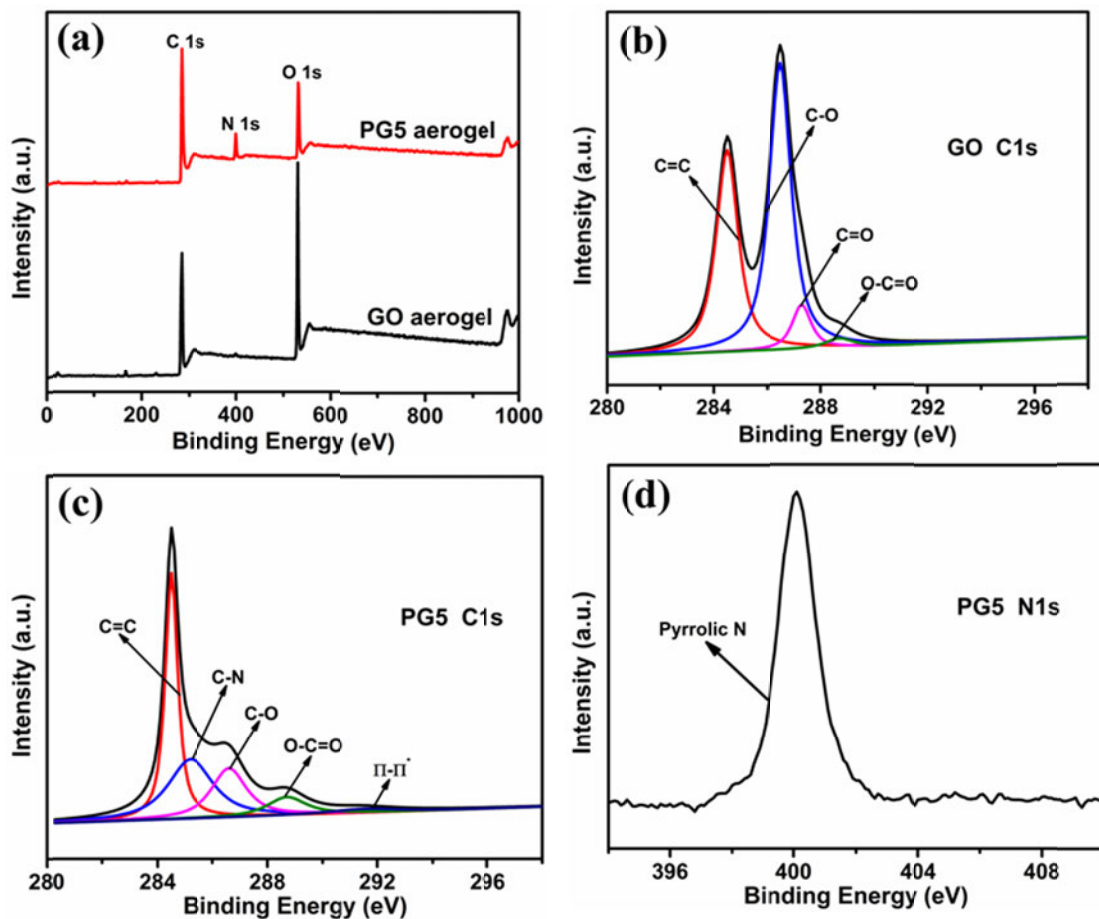


Fig. SI4 (a) XPS spectra of GO and rGO-PPy (PG5), (b) XPS spectra of C 1s of GO, (c) XPS survey spectra of C 1s of PG5 and (d) XPS spectra of N 1s of PG5.

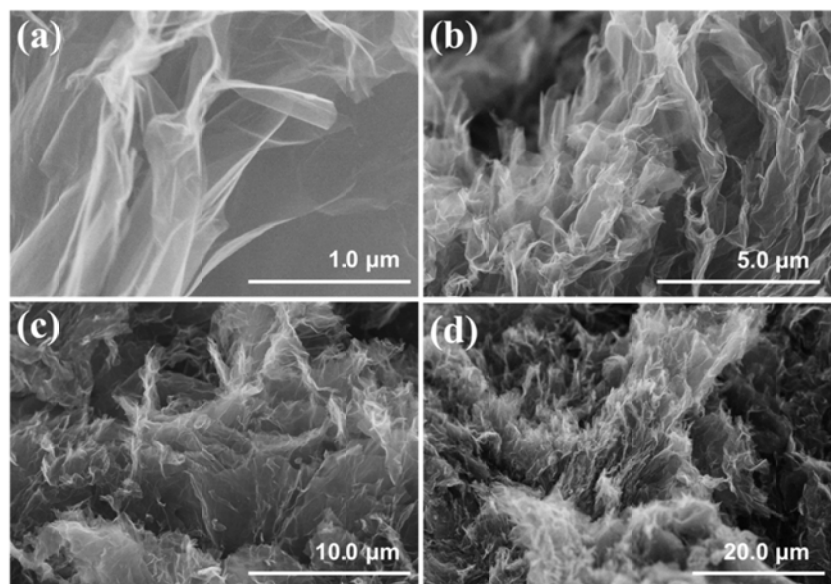


Fig. SI5 SEM images of rGO-PPy aerogels (PG5) with different magnifications.

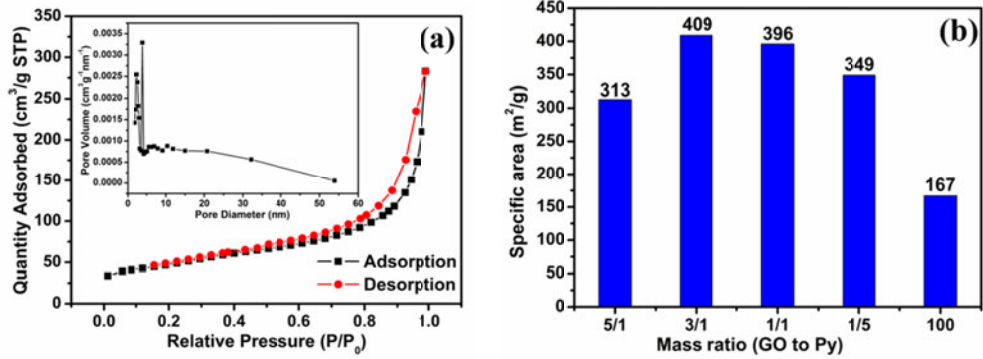


Fig. SI6 (a) Nitrogen adsorption-desorption isotherm of rGO aerogel. The insert is the corresponding pore-size distribution. (b) BET specific surface area of rGO-PPy aerogels with different mass ratio of GO to Py.

The type of hysteresis loop of rGO aerogel is vest to H4, indicating slit porous in rGO aerogel. The BET specific area 167 m<sup>2</sup>/g for rGO aerogel, which is much smaller than 408 m<sup>2</sup>/g of rGO-PPy aerogels (GP3). The pore-sizes mainly vest in 2.4 nm and 3.9 nm (the insert of Fig. SI5a), resulting from stacking and coalescing of rGO nanosheets, respectively. Furthermore, the BET specific surface area of rGO-PPy aerogels with different mass ratio of GO to Py have been investigated to explore the effect of mass ratio on BET specific surface area. As shown in Fig. SI5b, GP3 exhibits the highest BET specific area in all of the concerned aerogels, which attribute to the synergetic between GO and Py monomer. The existence of PPy polymerized by oxygen-containing groups of GO will effectively prevents the overlap of rGO nanosheets reduced by Py monomer. The maximized surface areas results from the best optimum combination of rGO and PPy.

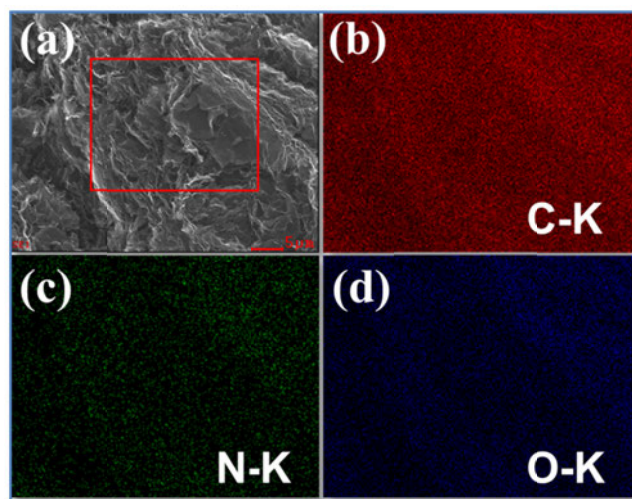


Fig. SI7 SEM-EDS spectra of rGO-PPy aerogel (PG5).

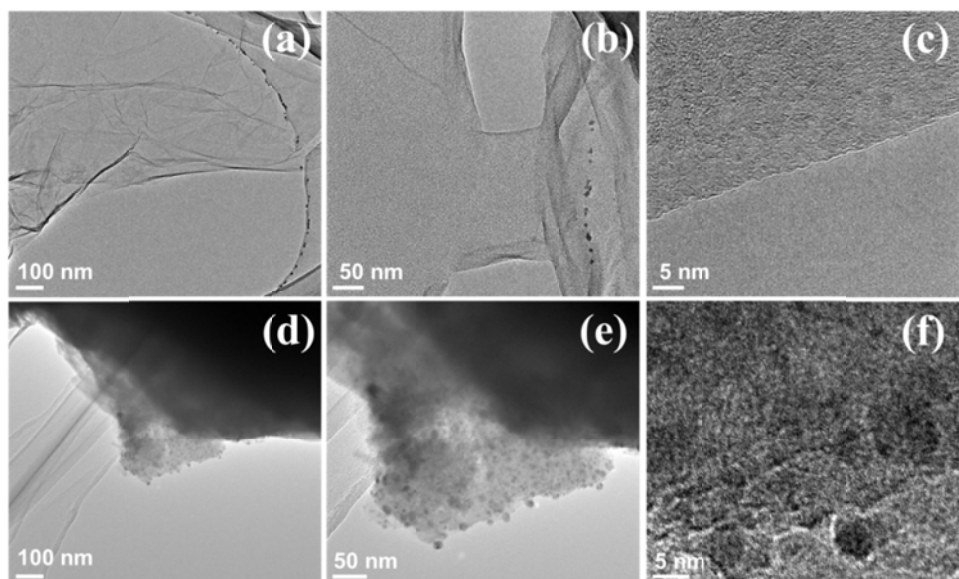


Fig. SI8 TEM images of GO nanosheets (a-c) and the rGO-PPy aerogel (PG5) (d-f) at different magnifications.

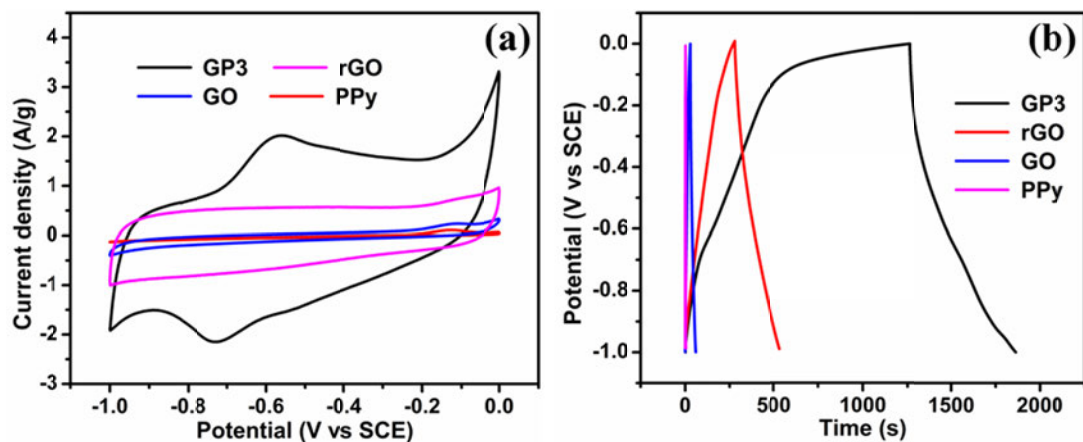


Fig. SI9 The CV curves of GP3, rGO, PPy aerogels and GO at the scan rate of 5 mV/s and (b) the galvanostatic charge-discharge curves of GP3, rGO, PPy aerogels and GO at the current density of 0.5 A/g in the potential range of -1~0 V vs SCE.

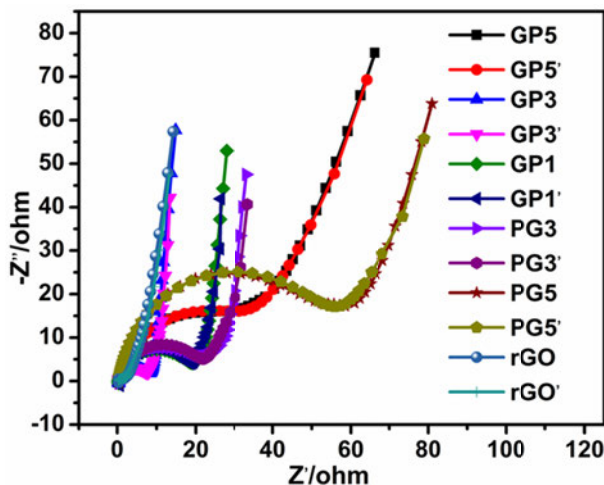


Fig. SI10 Nyquist plots of rGO-PPy aerogels and rGO aerogel with the fitting results matching by the equivalent circuit model in the insert of Fig. 6d by using Zview software.

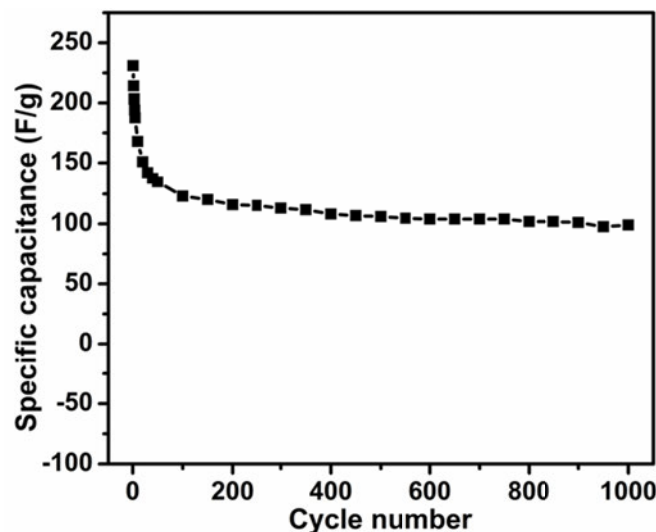


Fig. SI11 Cycle stability of GP3 aerogel during the long-term charge-discharge process at a current density of 1 A/g.

## Tables

Table SI1 Variation in the specific capacitance of rGO-PPy aerogels with different mass ratio of GO to Py. (Note: rGO aerogel has been made by L-ascorbic acid as the reducing agent)

Current density (A/g)	Samples				
	GP5	GP3	GP1	PG3	rGO
0.5	275.5	304	270	241.5	127.2
1	155.6	231	201.3	158.2	116.7
2	103.4	195.3	152	134.4	101.6
5	31.5	168.9	132.5	110	83
10	20	141.1	108	82.2	66

Table SI2 Rs and Rct values of various samples.

Samples	Rs	Rct
GP5	0.42327	37.94
GP3	0.34696	7.814
GP1	0.37685	18.89
PG3	0.39496	22.12
PG5	0.39984	56.22
rGO	0.3362	2.125

## References

- Y. F. Fan, Y. S. Liu, Q. Cai, Y. Z. Liu and J. M. Zhang, *Synthetic Met*, 2012, **162**, 1815-1821.
- K. E. Hnida, R. P. Socha and G. D. Sulka, *J Phys Chem C*, 2013, **117**, 19382-19392.